Journal of Molecular Structure 1121 (2016) 46–53

Contents lists available at ScienceDirect

Journal of Molecular Structure

journal homepage: http://www.elsevier.com/locate/molstruc

1-Formyl-3-phenyl-5-(4-isopropylphenyl)-2-pyrazoline: Synthesis, characterization, antimicrobial activity and DFT studies

Assia Sid [a], Amel Messai [b], Cemal Parlak [c], Nadide Kazancı [c], Dominique Luneau [d], Gürkan Keşan [e], Lydia Rhyman [f], Ibrahim A. Alswaidan [g], Ponnadurai Ramasami [f, *]

[a] Laboratoire des Sciences Analytiques Matériaux et Environnement (LSAME), Larbi Ben M'Hidi University, Oum El Bouaghi, 04000, Rue de Constantine, Algeria
[b] Laboratoire d'Ingénierie et Sciences des Matériaux Avancés (ISMA), Institut des Sciences et Technologie Abbès Laghrour University Khenchela, 40000, Algeria
[c] Department of Physics, Science Faculty, Ege University, Izmir, 35100, Turkey
[d] Laboratoire des Multimatériaux et Interfaces (UMR 5615), Université Claude Bernard Lyon 1, 69622, Villeurbanne Cedex, France
[e] Institute of Physics and Biophysics, Faculty of Science, University of South Bohemia, Branišovská 31, České Budějovice, 370 05, Czech Republic
[f] Computational Chemistry Group, Department of Chemistry, Faculty of Science, University of Mauritius, Réduit, 80837, Mauritius
[g] Department of Pharmaceutical Chemistry, College of Pharmacy, King Saud University, Riyadh, 11451, Saudi Arabia

ARTICLE INFO

Article history:
Received 2 March 2016
Received in revised form
12 May 2016
Accepted 12 May 2016
Available online 13 May 2016

Keywords:
Pyrazolines
Crystal structure
Hydrogen-bonding
Antimicrobial activity

ABSTRACT

The structure of 1-formyl-3-phenyl-5-(4-isopropylphenyl)-2-pyrazoline synthesized as single crystal was investigated by FTIR, NMR, XRD. Experimental data were complemented by quantum mechanical calculations. XRD data show that the compound crystallizes in the triclinic system (P−1) via trans isomer (a = 6.4267(4) Å, b = 10.9259(12) Å, c = 12.4628(9) Å and α = 102.894(8)°, β = 102.535(6)°, γ = 101.633(7)°). Anti-microbial screening results indicate that the compound shows promising activity. The theoretically predicted and experimentally obtained parameters reveal further insight into pyrazoline systems.

1. Introduction

α,β-unsaturated ketones especially chalcones as templates for the combinatorial assembly of heterocyclic compounds have been of research interests [1]. Pyrazolines have been widely used in the industry. They are employed as optical brightening agents, carrier transporting or emitting materials for textile, paper and fabrics. 2-Pyrazolines have higher hole-transport efficiency and some photoelectron characteristics. They are typical heterocyclic transition molecular crystals and have large molecular hyperpolarizability. This means that the photofractivity of the two-dimensional-array can be constructed with their nanoparticles in an applied optical field [2,3].

Numerous pyrazolines show various biological activities such as anti-microbial [4], anti-fungal [5], anti-depressant [6] and anti-convulsant [7]. 1-Thiocarbamoyl-3,5-diphenyl-2-pyrazolines [8] and their condensed analogs [9] and 1-n-substituted thiocarbamoyl-3-phenyl-5-thienyl-2-pyrazolines [10] have significant anti-convulsant and anti-depressant activities based on the Porsolt forced swimming test [11]. In addition, they are extensively useful as synthons in organic chemistry [12].

In 2011, the compound was synthesized by some of us [13] by reacting the appropriate chalcone with hydrazine hydrate. In the present study, the structure was confirmed by FTIR, NMR and single-crystal XRD. Hydrogen bonding interactions and antimicrobial activity of the compound were also investigated. As a supplement to the experimental investigations, density functional theory method in conjunction with the B3LYP functional and 6-31G(d,p) basis set was used to predict the structural and spectroscopic data of the compound in different medium.

2. Experimental

2.1. Synthesis

Chemicals were obtained from commercial sources. They were

* Corresponding author.
E-mail address: ramchemi@intnet.mu (P. Ramasami).

http://dx.doi.org/10.1016/j.molstruc.2016.05.043
0022-2860/

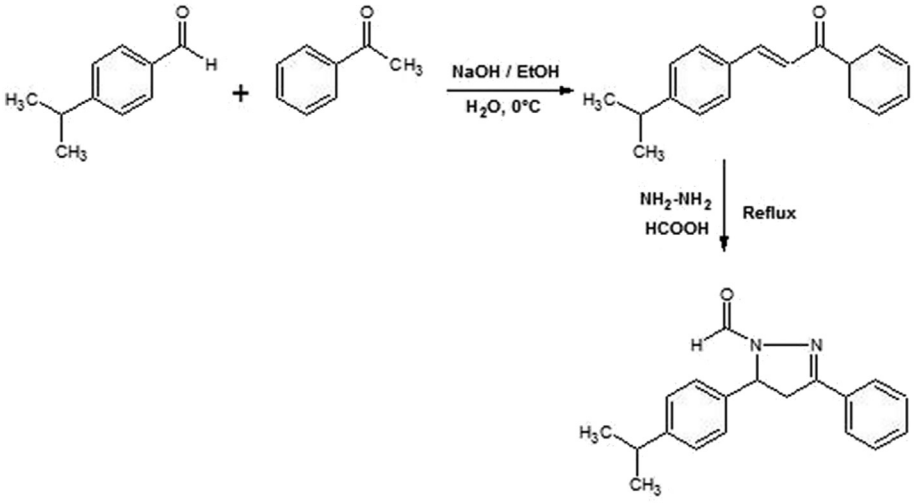

Fig. 1. Synthesis of 1-formyl-3-phenyl-5-(4-isopropylphenyl)-2-pyrazoline.

used without further purification and the path of reaction is illustrated in Fig. 1. A mixture of hydrazine hydrate (50 mmol), chalcone and formic acid (40 mL), prepared by aldol condensation of isopropyl benzaldehyde with acetophenone (10 mmol), was refluxed for 24h by constant stirring. The final solution was poured in water (100 mL) and allowed to stand. Crystals suitable for XRD were obtained from ethanol-toluene (1:1) mixture by the slow evaporation technique at room temperature (white crystal; yield 76%; mp 144–145 °C).

2.2. Instrumentation

A white block crystal of the compound with dimensions of 0.07 × 0.12 × 0.09 mm was selected and mounted on an Oxford Diffraction Xcalibur, Atlas, Gemini ultra diffractometer with Mo Kα radiation (λ = 0.71073 Å) and using ϕ and ψ scans at 293 K in the range of $3.0 < \theta < 29.2°$. CrysAlis was used for unit cell determination and reduction of data [14]. 6713 reflections were collected of which 3729 were independent while 2572 reflected with $I > 2\sigma(I)$. Structure was solved by direct method with SIR2004 [15] and refined by full-matrix least squares method on F^2 with SHELXL-1997 [16]. Both software are included within WinGX package [17]. Non-hydrogen and hydrogen atoms were anisotropically refined and located by Fourier map correspondingly. They were fixed in computed positions with distance constraints of C–H = 0.93 Å. Refinements converged at conventional R factor of 0.075 and Goodness-of-fit of 1.081. Maximum and minimum peaks in Fourier studies were 0.371 and −0.203 e $Å^{-3}$. ORTEP-3 [18] and MERCURY [19] were used to draw structural representations. Analysis was performed by PLATON [20], as incorporated in the WinGX [17]. FTIR spectrum (4000-400 cm^{-1}) was recorded by a NEXUS NICOLET Spectrometer by KBr pellet. ^1H and ^{13}C NMR

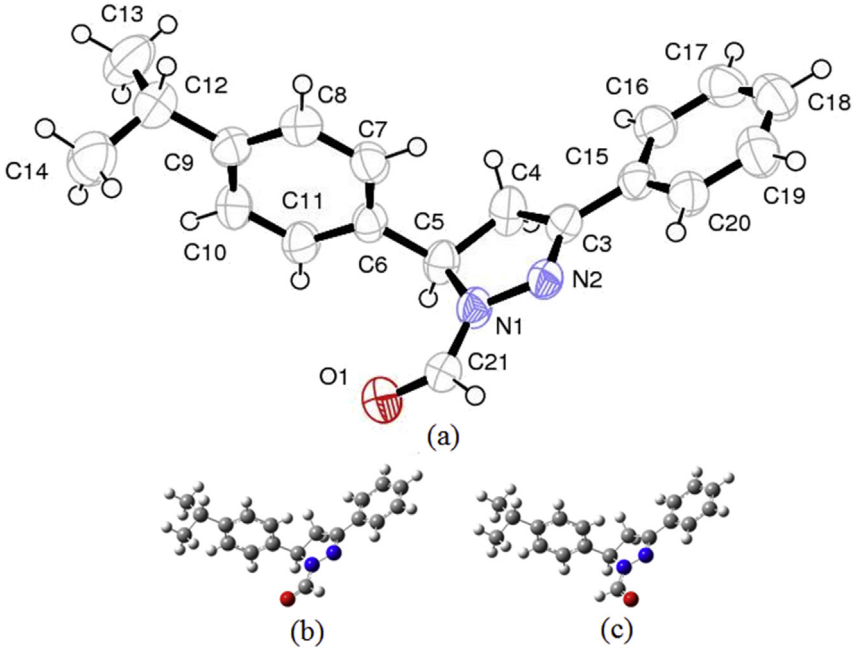

Figure 2. (a) Molecular view showing 50% probability thermal ellipsoids. Optimized structures of (b) trans and (c) cis isomers.

Table 1
Energetic parameters in the gas phase and different solvents.

Medium	Sum of electronic and thermal free energy (Hartree)		Relative energy (kcal/mol)		Mole fraction (%)	
	Trans	Cis	Trans	Cis	Trans	Cis
Gas phase	−920.520974	−920.515543	0	3.41	100	0
n-Hexane	−920.525484	−920.521012	0	2.81	100	0
n-Heptane	−920.525574	−920.521143	0	2.78	100	0
Cyclohexane	−920.525840	−920.521576	0	2.68	100	0
1,4-Dioxane	−920.526279	−920.522201	0	2.56	100	0
Benzene	−920.526409	−920.522353	0	2.55	100	0
Diethyl ether	−920.529028	−920.527163	0	1.17	88	12
Chloroform	−920.529413	−920.527463	0	1.22	89	11
Tetrahydrofuran	−920.530804	−920.528498	0	1.45	92	8
Dichloromethane	−920.531256	−920.528867	0	1.50	93	7
2-Butanol	−920.532318	−920.529969	0	1.47	92	8
2-Propanol	−920.532565	−920.530259	0	1.45	92	8
Acetone	−920.532631	−920.530330	0	1.44	92	8
Ethanol	−920.532826	−920.530575	0	1.41	92	8
Methanol	−920.533051	−920.530831	0	1.39	91	9
Acetonitrile	−920.533113	−920.530902	0	1.39	91	8
DMSO	−920.533267	−920.531074	0	1.38	91	8

spectra were reported in deuterated chloroform by Avance 400 Bruker spectrometer via TMS as internal standard.

2.3. Anti-microbial activity

Synthesized compound was screened *in vitro* for anti-bacterial and anti-fungal activities against *Escherchia coli*, *Salmonella typhi*, *Staphylococcus aureus, Bacillus subtilis* (200, 300, 400 500 μg/mL) and *Aspergillus niger*, *Aspergillus flavus*, *Pencillium chrysogenum, Fusirium moneliforme* (100, 200, 300, 400 μg/mL) via Agar Cup-Plate diffusion technique correspondingly. Concentrations were selected by detecting MIC of the molecule. DMSO diluted with water was used as solvent. Müller-Hinton and Sabouraud agars were used as the growth medium for the bacterial and fungal species correspondingly. DMSO was also used as a control for microorganisms. Activity against the strains of microorganisms was not showed at the control. Results were obtained after 48 h of incubation at 35 °C and 28–30 °C for anti-bacterial and anti-fungal tests, respectively. The zone of inhibition was measured in mm and they were compared with penicillin and griseofulvin for anti-bacterial and anti-fungal activities, respectively.

Table 2
Crystal parameters of the structure synthesized.

Parameter	Compound
Empirical formula	$C_{19}H_{20}N_2O$
Formula weight ($gmol^{-1}$)	292.37
Temperature (K)	293(2)
Crystal system	Triclinic
Space group	*P*−1
Hall symbol	-P 1
Unit cell dimensions (Å, °)	
a	6.4267(4)
b	10.9259(12)
c	12.4628(9)
α	102.894(8)
β	102.535(6)
γ	101.633(7)
Volume (A^3)	803.44(12)
Z[a]	2
Calculated density (g/cm^3)	1.209
Absorption coefficient (mm^{-1})	0.075
F(000)	312
Crystal size (mm^3)	0.09 × 0.04 × 0.01
Colour	White
Shape	Block
Cell parameters from	6713
Wavelength (Mo Kα) (Å)	0.71073
$\theta_{max} - \theta_{min}$	29.2°−3°
Measured reflections	6713
Independent reflections	3729
Reflections with $I > 2\sigma(I)$	2572
R_{int}	0.0309
Limiting indices	
h	−8 → 8
k	−15 → 14
l	−14 → 16
Refinement method	Full-matrix least-squares on F2
Final R indices[b] $[F^2 > 2\sigma(F^2)]$ R_1, wR_2	
Goodness-of-fit on F^2[c]	0.0750, 0.2474
Data/restraints/parameters	1.081
H atoms	3729/0/213
Largest difference peak and hole (e $Å^{-3}$)	a constrained refinement
$\Delta\rho_{max}$, $\Delta\rho_{min}$	0.371, −0.203

[a] The asymmetric unit contains 0.5 of the chemical formula.
[b] $R_1 = P|F_o - F_c|/F_o$. $wR_2 = \{P[w(F_o^2 - F_c^2)2]/P[w(F_o^2)^2]\}1/2$.
[c] $GOF = \{P[w(F_o^2 - F_c^2)^2]/(N_{obs} - N_{var})\}1/2$.

3. Computational method

Computations were carried out using Gaussian 09 [21] program. GaussView 5.0.8 was used for the structural and spectroscopic

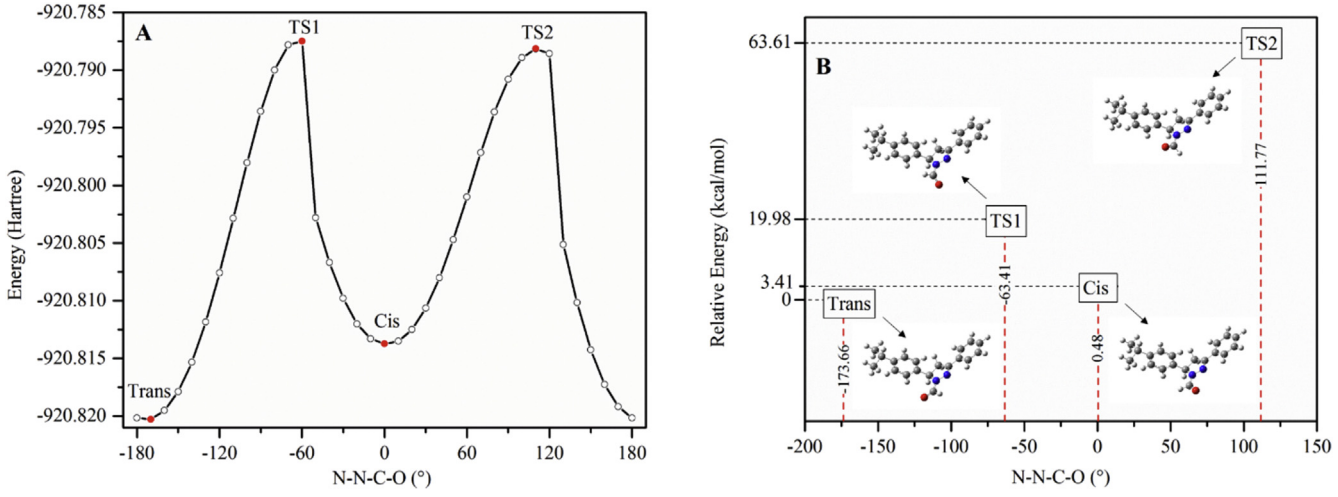

Figure 3. (A) PES scan and (B) transition state structures of the compound.

Table 3
Hydrogen bond lengths (Å) and angles (°).

D-H…A	D-H	H…A	D…A	D-H…A
C4-H4B···O1 ^{i}	1.02(5)	2.48(4)	3.470(5)	164(3)
C10-H10··· O1^{ii}	0.9300	2.4700	3.398(4)	175.00
C21-H21··· N2^{iii}	0.9900	2.5700	3.540(3)	166.00

Symmetry codes: (i) −1+x,y,z, (ii): 1−x,1−y,−z, (iii):1−x,1−y,1−z.

illustrations [22]. The geometrical structures of the conformers (Fig. 2) were optimized, without imposing symmetry, by the B3LYP functional together with 6-31G(d,p) basis set. In order to calculate the barrier of rotation, the transition state for the interconversion was also fully optimized. Further, potential energy surface (PES) analysis was performed by the rotations of NNCO torsion angle, scanning 360° with 10° increments.

Computations were carried out in the gas phase and different solvents. Polarizable continuum model was used to evaluate the solvent effect. Harmonic vibrational frequencies were computed using the same functional and basis set to confirm the nature of the ground state structure, and then scaled by 0.9627 [23]. Mole fractions of the individual conformers were calculated as described earlier [24–26].

4. Results and discussion

4.1. Energetic and structural analyses

Energetic parameters are given in Table 1. For the gas phase, the trans form is more stable than cis by 3.41 kcal/mol. The cis isomer has been neglected for the computation of equilibrium constant as energy difference is larger than 2 kcal/mol [24–26]. Hence, in the gas phase, the title compound prefers trans form with almost 100% probability. As can be observed from Fig. 3, the conformational preference is in agreement with the result found from PES analysis. Energy barriers for trans/cis forms to transition state structures (TS1/TS2) are 19.98/63.61 kcal/mol. In accordance with the mole fractions, the structure generally prefers the trans from with 100% probability for the non-polar solvents whereas the compound prefers cis and trans isomers in polar solvents with approximate probabilities of 7–12% and 88–93%, respectively. These conformational preferences are also agreement with the results obtained

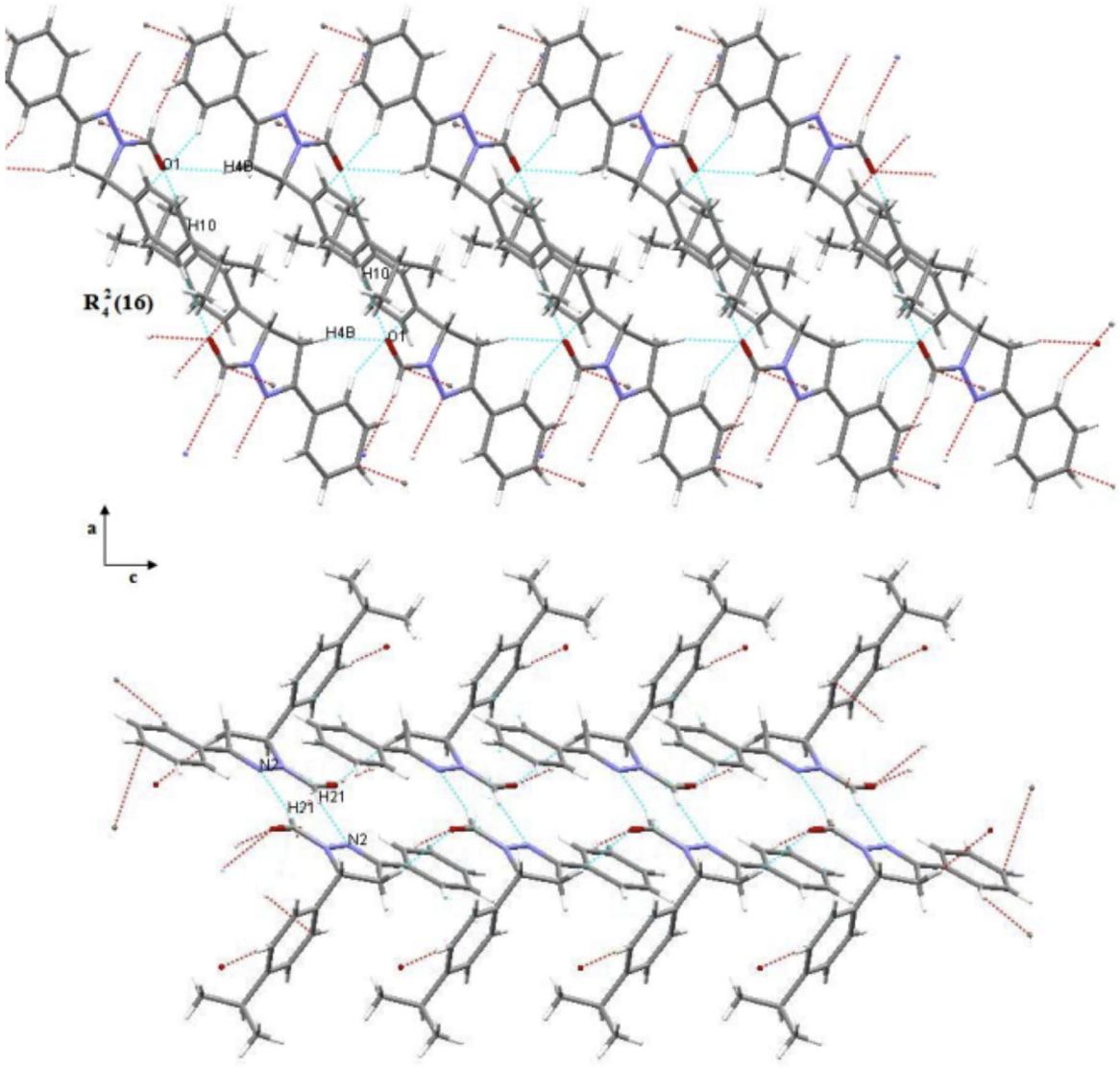

Fig. 4. The structure fragment.

Table 4
The structural parameters.

Bond lengths (A°)	Experimental	Calculated	Bond lengths (A)	Experimental	Calculated
O1–C21	1.220(4)	1.219	C8–C9	1.379(5)	1.402
N1–N2	1.385(3)	1.374	C9–C10	1.398(5)	1.401
N1–C5	1.486(3)	1.486	C9–C12	1.517(5)	1.523
N1–C21	1.334(4)	1.368	C10–C11	1.388(4)	1.401
N2–C3	1.287(4)	1.293	C12–C13	1.496(5)	1.540
C3–C4	1.510(4)	1.520	C12–C14	1.498(6)	1.540
C3–C15	1.472(4)	1.466	C15–C16	1.386(4)	1.404
C4–C5	1.536(5)	1.554	C15–C20	1.387(4)	1.408
C5–C6	1.510(4)	1.518	C16–C17	1.389(5)	1.395
C6–C7	1.386(5)	1.397	C17–C18	1.355(6)	1.394
C6–C11	1.383(4)	1.394	C18–C19	1.385(6)	1.399
C7–C8	1.384(5)	1.394	C19–C20	1.374(5)	1.390
Bond angles (°)			Bond angles (°)		
N2–N1–C5	113.3(2)	124.6	C8–C9–C10	117.0(3)	117.7
N2–N1–C21	120.5(2)	120.9	C8–C9–C12	121.0(3)	121.6
C5–N1–C21	126.3(2)	124.6	C10–C9–C12	122.0(3)	120.7
N1–N2–C3	108.3(2)	108.9	C9–C10–C11	121.4(3)	121.3
N2–C3–C4	113.6(3)	113.2	C6–C11–C10	121.2(3)	120.6
N2–C3–C15	121.0(2)	121.9	C9–C12–C13	111.0(3)	111.9
C4–C3–C15	125.5(3)	124.9	C9–C12–C14	112.6(3)	111.8
C3–C4–C5	103.1(2)	102.9	C13–C12–C14	113.1(3)	111.1
N1–C5–C4	100.7(2)	100.6	C3–C15–C16	119.8(2)	120.6
N1–C5–C6	110.6(2)	112.5	C3–C15–C20	121.5(3)	120.7
C4–C5–C6	115.2(3)	114.8	C16–C15–C20	118.8(3)	118.7
C5–C6–C7	121.2(3)	120.5	C15–C16–C17	120.4(3)	120.6
C5–C6–C11	121.6(3)	121.1	C16–C17–C18	120.2(3)	120.2
C7–C6–C11	117.2(3)	118.4	C17–C18–C19	120.1(4)	119.7
C6 –C7–C8	121.8(3)	120.8	C18–C19–C20	120.2(3)	120.4
C7–C8–C9	121.4(3)	121.1	O1–C21–N1	123.7(2)	123.4
Torsion angles (°)			Torsion angles (°)		
C5–N1–N2–C3	−5.9(3)	−2.9	C3–C4–C5–N1	−9.5(3)	−5.0
C21–N1–N2–C3	173.8(3)	169.8	C3–C4–C5–C6	109.5(3)	116.0
N2–N1–C5–C4	9.9(3)	5.1	N1–C5–C6–C7	66.0(4)	59.1
N2–N1–C5–C6	−112.4(3)	−117.5	N1–C5–C6–C11	−112.3(3)	−121.5
C21–N1–C5–C4	−169.7(3)	−167.3	C4–C5–C6–C7	−47.3(4)	−55.2
C21–N1–C5–C6	68.0(4)	70.0	C4–C5–C6–C11	134.4(3)	124.2
N2–N1–C21–O1	−179.5(3)	−173.7	C5–C6–C7–C8	−177.7(3)	179.2
C5–N1–C21–O1	0.1(5)	−1.7	C11–C6–C7–C8	0.7(5)	−0.3
N1–N2–C3–C4	−1.3(4)	−0.9	C5–C6–C11–C10	178.6(3)	−178.9
N1–N2–C3–C15	178.9(3)	179.7	C7–C6–C11–C10	0.2(4)	0.6
N2–C3–C4–C5	7.4(4)	4.0	C6–C7–C8–C9	−0.8(5)	−0.1
C15–C3–C4–C5	−172.8(3)	−176.6	C7–C8–C9–C10	−0.1(5)	0.3
N2–C3–C15–C16	176.4(3)	179.1	C10–C9–C12–C14	60.0(5)	63.3
N2–C3–C15–C20	−2.9(5)	−0.7	C9–C10–C11–C6	−1.1(5)	−0.4
C7–C8–C9–C12	−179.2(3)	−179.6	C3–C15–C16–C17	−179.6(3)	−179.8
C8–C9–C10–C11	1.0(5)	0.3	C20–C15–C16–C17	−0.2(5)	0.1
C12–C9–C10–C11	−179.9(3)	179.9	C3–C15–C20–C19	179.2(3)	179.8
C8–C9–C12–C13	111.1(4)	−62.1	C16–C15–C20–C19	−0.1(5)	−0.04
C8–C9–C12–C14	−120.9(4)	63.3	C15–C16–C17–C18	0.3(5)	−0.03
C10–C9–C12–C13	−68.0(4)	−62.1	C16–C17–C18–C19	−0.2(5)	0.01
C4–C3–C15–C16	−3.4(5)	−0.18	C17–C18–C19–C20	−0.1(6)	−0.01
C4–C3–C15–C20	177.3(3)	−180.0	C18–C19–C20–C15	0.3(5)	0.03

from XRD analysis.

Crystal parameters of the structure are collected in Table 2. Further, equivalent thermal parameters are presented in Table SI1 together with atomic coordinates. Molecular structure with atom-numbering is illustrated in Fig. 2. Crystal packing view is also given in Fig. SI1. The refinement details are available in the CCDC: 1429353. Synthesized molecule consists of discrete [C_3H_7-$PhC_3H_2N_2CHOPh$] entities. It crystallizes in triclinic system by *P*-1 space group. Unit cell parameters are a = 6.4267(4) Å, b = 10.9259(12) Å, c = 12.4628(9) Å and α = 102.894(8)°, β = 102.535(6)°, γ = 101.633(7)°. The compound exists in a trans configuration (Fig. 2a). Average mean plane angles between the pyrazolinyl ring with phenyl at positions 3 and 5 of pyrazoline are 5.4° and 88.6°, correspondingly. The average mean plane angle is 6.3° between the formyl group and pyrazoline ring. These values compare satisfactorily to similar compounds in the literature [27–30]. All the bond lengths and angles in the phenyl rings are in the expected range. In the pyrazolinyl ring, the C=N, C–N and N–N (1.287(4), 1.486(3) and 1.385(3)) Å bond lengths are all similar to those found in analogous structures (C=N: 1.291(2)–1.300(10) Å, C–N: 1.482(2)–1.515(9) Å and N–N: 1.373(2)–1.380(8) Å) [30,31]. Crystal packing is mainly consolidated by C–H … O and C–H … N intra- or inter-molecular hydrogen bonds. Information of three hydrogen bonds is given in the asymmetric unit (Table 3). Each O1 atom is connected to two adjacent discrete molecules through C4-H4B … O1 (symmetry code: -1+x,y,z) hydrogen bond of 3.470(5) Å and C10-H10 … O1 (symmetry code: 1−x, 1−y,−z) hydrogen bond of 3.398(4) Å. Packing suggests that rings show how the neighboring moieties link to each other through the C4-H4B … O1 and C10-H10 … O1 interactions. These rings are connected yielding to infinite supramolecular cycles (Fig. 4). Further, the N2 atom is involved in an intramolecular C21-H21 … N2 (symmetry code:

Table 5
Some parameters of the compound (P (ε) = (ε−1)/(ε+2)).

Medium		B3LYP/6-31G(d,p)			
		Trans isomer			
	P(ε)	Dipole moment	C=O bond length	ν(C=O)	Scaled ν(C=O)
Gas phase	–	4.10	1.219	1786.61	1719.97
n-Hexane	0.227	4.77	1.221	1775.00	1708.79
n-Heptane	0.239	4.79	1.221	1774.57	1708.38
Cyclohexane	0.253	4.83	1.221	1773.65	1707.49
1,4-Dioxane	0.287	4.91	1.222	1772.03	1705.93
Benzene	0.298	4.93	1.222	1771.55	1705.47
Diethyl ether	0.519	5.36	1.224	1761.99	1696.27
Chloroform	0.553	5.42	1.224	1760.75	1695.07
Tetrahydrofuran	0.682	5.63	1.225	1756.11	1690.61
Dichloromethane	0.726	5.70	1.225	1754.66	1689.21
2-Butanol	0.833	5.86	1.226	1751.24	1685.92
2-Propanol	0.859	5.89	1.226	1750.41	1685.12
Acetone	0.867	5.91	1.226	1750.19	1684.91
Ethanol	0.888	5.94	1.226	1749.56	1684.30
Methanol	0.913	5.97	1.226	1748.83	1683.60
Acetonitrile	0.920	5.98	1.226	1748.63	1683.41
DMSO	0.939	6.00	1.226	1748.11	1682.91

Table 6
Anti-bacterial screening results.

Compound	*Escherchia coli*	*Salmonella typhi*	*Staphylococcus aureus*	*Bacillus subtilis*
Bis-Pyr	15	20	16	08
Penicillin	18	25	40	17
DMSO	–	–	–	–

-: No antibacterial activity.

1−x,1−y, 1−z) hydrogen bonding of 3.540(3) with forming a dimer (Fig. 4). The calculated parameters (H21···N2: 2.489 Å, ∠C21H21N2: 153.9°) are in good agreement with the experimentally observed values (H21…N2: 2.570 Å, ∠C21H21N2: 166.0°) for the intramolecular hydrogen bond.

The structural parameters are given in Table 4. In general, all calculated parameters are in good agreement with the experimental data. Largest difference between the experimental and theoretical bond length (angle) is 0.044 Å; C12-C13 (11.3°; N2-N1-C5). Mean absolute deviations between the theoretical and experimental bond lengths and angles are found to be 0.015 Å and 1.0°.

4.2. Spectroscopic studies

FTIR spectrum is carried out to analyze the chemical bonding and structure (Fig. SI2). It shows a strong band for ν(C=O) at 1658 cm^{-1}. The theoretical value (ν_{21} by B3LYP/6-31G(d,p)) is calculated as 1720 cm^{-1}. The carbonyl stretching frequency is consistent with previously reported for 1-acetyl-3-(2,4-dichloro-5-fluoro-phenyl)-5-phenyl-pyrazoline where the experimental band was observed as 1660 cm^{-1} whereas the theoretical data (B3LYP/6-31G(d)) was computed as 1708 cm^{-1} [30]. C=N stretching vibration is observed at 1596 cm^{-1} whereas the N–N stretching band together with the pyrazoline ring CH contribution is shown at 1156 cm^{-1}. The corresponding theoretical data (ν_{26} and ν_{57}) are computed as 1565 and 1121 cm^{-1}, respectively. All computed vibrational frequencies and their intensities are tabulated in Table SI2.

The calculated carbonyl stretching frequencies of the compound are collected in Table 5. As shown in Table 5, significant changes in the carbonyl stretching modes of the compound are observed when considering the solutions. For n-hexane, the C=O stretching is computed at higher frequencies. Since there is no any remarkable solute-solvent interaction for inert solvent n-hexane, it belongs to the free monomer state for C=O. These bands are found at lower frequency in polar solvents. The C=O bond lengths increase by increasing dielectric constant of solvent. Therefore, the C=O stretching frequency should decrease. It is definitely shown in Table 5 that these requirements are fulfilled. The frequency shift is clarified by positive character increased on O atom in polar solvents. Further, there is linear correlation between the dipole moment and dielectric constant.

In the ^{1}H NMR spectrum, the tree H atoms attached to the C4 and C5 atoms of the heterocyclic ring have given an ABX spin system and a doublet signal at 8.96 ppm. It refers to the presence of *N*-formyl. The values of chemical shift and coupling constant measured prove 2-pyrazoline in structure. In the ^{13}C NMR spectra (Fig. SI3), chemical shifts of carbon atoms C3 at 155.85 ppm, C4 at 42.60 ppm and C5 at 58.80 ppm corroborate 2-pyrazoline structure determined by ^{1}H NMR. Chemical shift of C3 is consistent with previously reported for 1-formyl-3-phenyl-Δ^{2}-pyrazoline as 157.34 ppm [29]. C5 is easily differentiated from C4. The C4 and C5

Table 7
Anti-fungal screening results.

Compound	*Aspergillus niger*	*Aspergillus flavus*	*Pencillium chrysogenum*	*Fusirium moneliforme*
Bis-Pyr	–	+	+	+
Greseofulvin	–	–	–	–
Control	+	+	+	+

Table 8
Gas phase molecular orbital energies (eV) and dipole moment (Debye).

Parameters	Trans	Cis
HOMO	−5.82	−5.77
LUMO	−1.40	−1.34
HOMO-LUMO Gap	4.42	4.43
Dipole moment	4.10	5.78

chemical shifts were reported as 31.79 and 42.46 ppm for 1-formyl-3-phenyl-Δ^2-pyrazoline [29] while they appeared at 32 and 47 ppm in 3-phenyl-*N*-arylpyrazolines [32]. However, the chemical shifts of the C4 and C5 in the current work increase due to the different chemical environment. ^{13}C NMR chemical shifts for *N*-formyl of the molecule are assigned at 160.10 ppm. Similar chemical shift is also observed as 160.24 ppm for the 1-formyl-3-phenyl-Δ^2-pyrazoline [29]. All other chemical shifts are the same with previously reported [13].

4.3. Anti-microbial activity

The antimicrobial screening results are collected in Tables 6 and 7 and the results indicate that the synthesized compound shows promising and good activities against *Escherchia coli* and *Salmonella typhi* correspondingly. However, it gives low activities against *Staphylococcus aureus* and *Bacillus subtilis*. Compound has no effect against *Aspergillus niger*, but it shows inhibitory effects against *Aspergillus flavus*, *Pencillium chrysogenum* and *Fusirium moneliforme* which probably indicates that the synthesized product has a specific effect on those microorganisms. It is reported in literature that molecular orbital energy and dipole moment may be related to biological activity [33]. Therefore, we calculated these parameters and they are summarised in Table 8. These energies and dipole moment are sufficient for the compound to be biologically active when compared with analogous derivatives [33,34].

5. Conclusions

Structural investigation of 1-formyl-3-phenyl-5-(4-isopropylphenyl)-2-pyrazoline was successfully conducted by FTIR, NMR, XRD and quantum mechanical calculations. Anti-microbial activity of the compound is also reported. As a consequence, the compound crystallizes in the triclinic system (P−1) by two molecules in the asymmetric unit. The trans isomer is the most stable and there is high interconversion energy barrier which is independent on the solvent. Crystal packing is mainly consolidated by C−H…O and C−H…N intra-molecular H-bonds and resulting in infinite chains obtained by $R_4^2(16)$ rings and $D_2^2(8)$ dimer. The C=O stretching vibration is decreasing with increasing solvent polarity, whereas its bond length and dipole moment is upward tendency. The compound in all medium has large dipole moment (4.1 Debye) which is an essential criterion for drug-receptor interaction [35]. Compound shows promising and good activities against *Escherchia coli* and *Salmonella typhi* correspondingly.

Acknowledgements

AM and DL acknowledge the Tassili Programme N° 15MDU940 for the financial support. The authors are thankful to reviewers for their useful comments to improve the manuscript. The authors extend their appreciation to the Deanship of Scientific Research at King Saud University for the research group Project No. RGP VPP-207.

Appendix A. Supplementary data

Supplementary data related to this article can be found at http://dx.doi.org/10.1016/j.molstruc.2016.05.043.

References

[1] (a) D.G. Powers, D.S. Casebier, D. Fokas, W.J. Ryan, J.R. Troth, D.L. Coffen, Automated parallel synthesis of chalcone-based screening libraries, Tetrahedron 54 (1998) 4085–4096;
(b) D. Fokas, W.J. Ryan, D.S. Casebier, D.L. Coffen, Solution phase synthesis of a spiro[pyrrolidine-2,3′-oxindole] library via a three component 1,3-dipolar cycloaddition reaction, Tetrahedron Lett. 39 (1998) 2235–2238.
[2] J.S. Yin, Z.L. Wang, Ordered self-assembling of tetrahedral oxide nanocrystals, Phys. Rev. Lett. 79 (1997) 2570–2573.
[3] K. Ramalingam, G.X. Thyvelikakath, K.D. Berlin, R.W. Chesnut, R.A. Brown, N.N. Durham, S.E. Ealick, D. Van der Helm, Synthesis and biological activity of some derivatives of thiochroman-4-one and tetrahydrothiapyran-4-one, J. Med. Chem. 20 (1977) 847–850.
[4] T. Sano, T. Fujii, Y. Nishio, Y. Hamada, K. Shibata, K. Kuroki, Pyrazoline dimers for hole transport materials in organic electroluminescent devices, Jpn. J. Appl. Phys. 34 (1995) 3124–3127.
[5] S.S. Korgaokar, P.H. Patel, M.J. Shah, H.H. Parekh, Studies on pyrazolines: preparation and antimicrobial activity of 3-(3â€™(P-Chlorophenylsulphonamidophenyl)-5 Aryl-1H/Acetyl pyrazolines, Ind. J. Pharm. Sci. 58 (1996) 222–225.
[6] Y.R. Prasad, A.L. Rao, L. Prasoona, K. Murali, P.R. Kumar, Synthesis and antidepressant activity of some 1,3,5-triphenyl-2-pyrazolines and 3-(2″-hydroxy naphthalen-1″-yl)-1,5-diphenyl-2-pyrazolines, Bioorg. Med. Chem. Lett. 15 (2005) 5030–5034.
[7] S.S. Parmar, B.R. Pandey, C. Dwivedi, R.D. Harbison, Anticonvulsant sant activity and monoamine oxidase inhibitory properties of 1,3,5-trisubstituted pyrazolines, J. Pharm. Sci. 63 (1974) 1152–1155.
[8] A.A. Bilgin, E. Palaska, R. Sunal, Studies on the synthesis and antidepressant activity of some 1-thiocarbamoyl-3,5-diphenyl-2-pyrazolines, Arzneim. Forsch. (Drug Res.) 43 (1993) 1041–1042.
[9] A.A. Bilgin, A. Yesilada, E. Palaska, R. Sunal, Synthesis and antidepressant activity of some new 8-thiocarbamoyl-7,8-diazabicyclo (4.3.0) non-6-ene derivatives, Arzneim. Forsch. (Drug Res.) 42 (1992) 1271–1273.
[10] A. Yesilada, G. Uçar, K. Erol, A.A. Bilgin, 1-N-substitued thiocarbamoyl-3-phenyl-5-thienyl-2-pyrazolines: synthesis and evaluation as MAO inhibitors, Arch. Pharm. Pharm. Med. Chem. 336 (2003) 362–371.
[11] R.D. Porsolt, A. Bertin, M. Jalfre, Behavioural despair in mice: a primary screening test for antidepressants, Arch. Int. Pharmacodyn. 229 (1977) 327–336.
[12] L.C. Behr, F. Fusco, C.H. Jarboe, Pyrazoles, Pyrazolines, Pyrazolidines,Indazoles and Condensed Rings, Wiley, New York, 1967.
[13] A. Sid, K. Lamara, M. Mokhtari, N. Ziani, P. Mosset, Synthesis and characterization of 1-formyl-3-phenyl-5-aryl-2-pyrazolines, Eur. J. Chem. 2 (2011) 311–313.
[14] Oxford Diffraction Xcalibur CCD system, CrysAlis Software System, Version 1.171, Oxford Diffraction Ltd., Abington, 2006.
[15] M.C. Burla, R. Caliandro, M. Camalli, B. Carrozzini, G.L. Cascarano, L. De Caro, C. Giacovazzo, G. Polidori, R. Spagna, SIR2004: an improved tool for crystal structure determination and refinement, J. Appl. Cryst. 38 (2005) 381–388.
[16] G.M. Sheldrick, SHELXL97, University of Göttingen, Germany, 1997.
[17] L.J. Farrugia, WinGX suite for small-molecule single-crystal crystallography, J. Appl. Cryst. 32 (1999) 837–838.
[18] L.J. Farrugia, ORTEP-3 for windows - a version of ORTEP-III with a graphical user interface (GUI), J. Appl. Cryst. 30 (1997) 565.
[19] I.J. Bruno, J.C. Cole, P.R. Edgington, M. Kessler, C.F. Macrae, P. McCabe, J. Pearson, R. Taylor, New software for searching the Cambridge structural database and visualizing crystal structures, Acta Cryst. B 58 (2002) 389–397.
[20] A.L. Spek, Single-crystal structure validation with the program PLATON, J. Appl. Cryst. 36 (2003) 7–13.
[21] M.J. Frisch, G.W. Trucks, H.B. Schlegel, et al., Gaussian 09, Revision A.1, Gaussian Inc., Wallingford, CT, 2009.
[22] R.D. Dennington, T.A. Keith, J.M. Millam, GaussView 5.0.8, Gaussian Inc., 2008.
[23] J.P. Merrick, D. Moran, L. Radom, An evaluation of harmonic vibrational frequency scale factors, J. Phys. Chem. 111 (2007) 11683–11700.
[24] Ö. Alver, C. Parlak, DFT, FT-Raman, FT-IR, liquid and solid state NMR studies of 2,6-dimethoxyphenylboronic acid, Vib. Spectrosc. 54 (2010) 1–9.
[25] M. Tursun, G. Keşan, C. Parlak, M. Şenyel, Vibrational spectroscopic investigation and conformational analysis of 1-heptylamine: a comparative density functional study, Spectrochim. Acta A 114 (2013) 668–680.
[26] C. Parlak, Theoretical and experimental vibrational spectroscopic study of 4-(1-Pyrrolidinyl)piperidine, J. Mol. Struct. 966 (2010) 1–7.
[27] B. Duffin, The crystal structure of di-phenyl-Δ^2-pyrazoline, Acta Cryst. B 24 (1968) 1256–1261.
[28] R.V. Krishnakumar, S. Natarajan, V. Vijayabaskar, S. Perumal, Racemic 1-Acetyl-5-phenyl-3-styryl-2-pyrazoline, Acta Cryst. C 54 (1998) 976–978.
[29] I. Alkorta, J. Elguero, A. Fruchier, N. Jagerovic, G.P.A. Yap, The structure of 1-formyl-3-phenyl-Δ^2-pyrazoline in the gas phase (DFT calculations), in

solution (NMR) and in the solid state (X-ray crystallography), J. Mol. Struct. 689 (2004) 251–254.
[30] F. Jian a, P. Zhao, H. Guo, Y. Li, Synthesis, characterization, crystal structure and DFT studies on 1-acetyl-3-(2,4-dichloro-5-fluoro-phenyl)-5-phenyl-pyrazoline, Spectrochim. Acta Part A 69 (2008) 647–653.
[31] C.J. Fahrni, L.C. Yang, D.G. VanDerveer, Tuning the photoinduced electron-transfer thermodynamics in 1,3,5-triaryl-2-pyrazoline fluorophores: X-ray structures, photophysical characterization, computational analysis, and in vivo evaluation, J. Am. Chem. Soc. 125 (2003) 3799–3812.
[32] R. Faure, J. Llinares, E.J. Vincent, J. Elguero, Etude en résonance magnétique nucléaire du carbone-13 de n-Aryl pyrazolines-2 diversement substituées. Effets de substituant et etude conformationnelle, Org. Magn. Res. 12 (1979) 579–582.
[33] S.A. Khan, A.M. Asiri, S. Kumar, K. Sharma, Green synthesis, antibacterial activity and computational study of pyrazoline and pyrimidine derivatives from 3-(3,4-dimethoxy-phenyl-1-(2,5-dimethyl-thiophen-3-yl)-propenone, Eur. J. Chem. 5 (2014) 85–90.
[34] F. Lamchouri, H. Toufik, S.M. Bouzzine, M. Hamidi, M. Bouachrine, Experimental and computational study of biological activities of alkaloids isolated from Peganum harmala seeds, J. Mater. Environ. Sci. 1 (2010) 343–352.
[35] R. Hoffmann, P.v.R. Schleyer, H.F. Schaefer, Predicting molecules - more realism, please!, Angew. Chem. Int. Ed. 47 (2008) 7164–7167.